Food & Function

ROYAL SOCIETY OF CHEMISTRY

PAPER

View Article Online
View Journal | View Issue

Cite this: *Food Funct.*, 2023, **14**, 7692

Nobiletin protects against ferroptosis to alleviate sepsis-associated acute liver injury by modulating the gut microbiota†

Wei Huang,[a] Hui Chen,[a] Qi He,[b] Weidang Xie,[a] Zanlin Peng,[a] Qiang Ma,[c] Qiaobing Huang,[b] Zhongqing Chen*[a] and Yanan Liu *[a]

Nobiletin (NOB), a plant-based polymethoxyflavone, is a promising protective agent against sepsis; yet the mechanisms were not fully elucidated. The gut microbiota is found to be strongly associated with sepsis-associated acute liver injury (SALI). Here, our study aimed to evaluate the protective effect of NOB on SALI and explore the underlying molecular mechanisms. Cecal ligation and puncture (CLP) was used to induce SALI in mice. NOB was administered by gavage for 7 days before CLP induction. The 16S rRNA gene sequencing and fecal microbiota transplantation (FMT) were performed to verify the function of the gut microbiota. The markers of ferroptosis, inflammation, gut microbiota composition, and liver injury were determined. NOB administration significantly alleviated hepatic ferroptosis and inflammation in septic mice. Meanwhile, NOB upregulated the expression levels of nuclear factor E2-related factor 2 (Nrf2) and its downstream protein heme oxygenase-1 (HO-1). The protective effect of NOB administration against ferroptosis in SALI mice was reversed by the Nrf2 inhibitor ML385. Additionally, increased abundances of *Ligilactobacillus*, *Akkermansia*, and *Lactobacillus*, and decreased abundances of *Dubosiella* and *Bacteroides* in the gut were observed under NOB administration, suggesting that NOB might modulate the gut microbiota composition of septic mice. Furthermore, gut microbiota ablation by antibiotic treatment partly reversed the protective effects of NOB on sepsis. FMT also confirmed that NOB inhibited ferroptosis and activated Nrf2 signalling in SALI mice by modulating the gut microbiota. These results revealed that, by modulating the gut microbiota, NOB attenuated ferroptosis in septic liver injury through upregulating Nrf2–Gpx4. Our findings provide novel insights into microbiome-based therapeutic approaches for sepsis.

Received 26th April 2023,
Accepted 9th July 2023

DOI: 10.1039/d3fo01684f

rsc.li/food-function

1. Introduction

Sepsis is a life-threatening organ dysfunction characterized by overwhelming inflammation and aberrant immune responses with high morbidity and mortality.[1] Indeed, more than 1.5 million patients suffer from sepsis per year, attributing to approximately 33% mortality in the USA.[2] Uncontrolled inflammation induces inflammatory storms, and subsequently multiple organ dysfunction syndromes (MODS).[3] As the liver is a critical organ to balance the host homeostasis and regulate the host-defense effect, liver dysfunction and failure have a critical effect on the severity and outcome of sepsis.[4,5] Unfortunately, the development of clinically feasible therapeutic methods is limited to date. Given the dangers of sepsis-associated acute liver injury (SALI), improved knowledge of the pathogenesis of SALI might contribute to finding novel treatment approaches for sepsis.

Ferroptosis is a programmed cell death, mainly driven by iron-dependent lipid peroxidation, which plays an important role in the pathogenesis of various types of liver diseases.[6] To date, multiple pharmacological or natural compounds and cell-intrinsic proteins have been found to regulate and affect the process and function of ferroptosis.[7,8] Specifically, glutathione peroxidase 4 (Gpx4) plays a central role in regulating the glutathione (GSH) antioxidant system and inhibiting ferroptosis by converting lipid hydroperoxides into nontoxic lipid alcohols.[9] Meanwhile, growing evidence indicates that SALI leads to ferroptosis *via* iron overload, lipid peroxidation, and

[a]*Department of Critical Care Medicine, Nanfang Hospital, Southern Medical University, Guangzhou, China. E-mail: zhongqingchen2008@163.com, lyn21100145@i.smu.edu.cn*
[b]*Guangdong Provincial Key Laboratory of Cardiac Function and Microcirculation, Southern Medical University, Guangzhou, China*
[c]*Department of Biopharmaceutics, School of Laboratory Medicine and Biotechnology, Southern Medical University, Guangzhou, China*
† Electronic supplementary information (ESI) available. See DOI: https://doi.org/10.1039/d3fo01684f

redox imbalance.[10,11] Thus, targeting ferroptosis may serve as a promising novel therapeutic strategy for SALI. Nuclear factor E2-related factor 2 (Nrf2), a transcription factor, is the major regulator of the cellular antioxidant response and plays a critical role in regulating lipid peroxidation and iron metabolism in the regulation of ferroptosis.[12] Recently, certain studies have clarified that Nrf2/Gpx4 activation prevents lipopolysaccharide (LPS)/D-GalN-induced acute liver injury and inhibits ferroptosis.[13] Hence, we explore here the feasibility of targeting Nrf2 to attenuate ferroptosis in SALI.

The gut microbiota is increasingly recognized as a chief regulator of immune activities in the gut and extra-gut organs, and remotely modulates multiple organ injuries distant from the gut.[14] Intestinal dysbiosis and intestinal barrier failure promote pathogenic microbial overgrowth and translocation of intestinal pathogen-associated molecular patterns (PAMPs) to the lymphatic and portal systems, impairing the body's defense against infection or injury and aggravating organ damage during sepsis.[15] Moreover, gut microbiome alterations play crucial roles in the progression of SALI.[16] It has been reported that disrupted composition and function of the gut microbiota during sepsis contribute to sepsis-linked organ dysfunction through the gut–liver axis.[17] Gong *et al.* demonstrated recently that the gut microbiota metabolite granisetron protected mice against sepsis-induced liver injury.[18] Another study has indicated that gut microbiota-derived indole-3-propionic acid could mediate the susceptibility of sepsis-induced liver injury by modulating the intestinal microbiota.[19] Hence, maintaining gut microbiota homeostasis may be a therapeutic strategy for SALI. In addition, a study shows that the gut microbiota metabolite capsiate can protect the intestine from ischemia/reperfusion (I/R) injury by inhibiting ferroptosis.[20] The gut microbiota metabolite glycochenodeoxycholate leads to inflammation and lipid metabolism disorder by triggering ferroptosis in response to environmental toxins.[21] It is found that inflammation-associated sepsis can affect iron homeostasis and increase intestinal permeability by mediating gut microbiota dysbiosis.[22–24] Therefore, studies investigating the roles played by the gut microbiota in regulating ferroptotic signalling in SALI are inspiring and profound.

Nobiletin (NOB) is a polymethoxylated flavone extracted from citrus peels that possess multiple health-promoting properties, highlighting its protective role in anti-inflammatory, potential inhibition of oxidative stress, immunomodulatory, antiatherosclerosis, and antidiabetic effects.[25–27] Moreover, oral gavage of NOB has been shown to improve intestinal metabolism and modulate the gut microbiota.[28] NOB treatment modulates the gut microbiota components and particularly increases *Akkermansia* and *Bacteroides* abundance for activating thermogenesis in brown and beige adipocytes to prevent high-fat diet-induced obesity.[29] Zhang *et al.* reported that NOB administration could modify the gut microbiota by enhancing the abundance of *Allobaculum* and *Roseburia* with improved demethylation ability and increased production of short-chain fatty acids.[30] Meanwhile, Lo *et al.* demonstrated that NOB ameliorated renal fibrosis by preventing ferroptosis and oxidative stress in a chronic kidney disease (CKD) mouse model.[31] Given that NOB is becoming recognized as both affecting the gut microbiota and causing liver injury, in our study, we aimed to investigate a possible causal relationship among the gut microbiota composition, sepsis-induced ferroptosis, and protective role of NOB in SALI, with the hope of providing a therapeutic strategy for sepsis.

2. Materials and methods

2.1 Animal treatment

All animal experimental procedures were performed strictly following the Guide for the Care and Use of Laboratory Animals (US National Institutes of Health, Bethesda, MD, USA) and were approved by the Institutional Animal Care and Use Committee of Nanfang Hospital of Southern Medical University (Approved ID: NFYY-2021-0364). Specific pathogen-free male C57BL/6 mice (6 to 8 weeks old) were used and purchased from the animal center of Southern Medical University. All mice were housed under temperature-controlled conditions with a 12/12-hour light–dark cycle with free access to food and water. The model of sepsis was established by cecal ligation and puncture (CLP) treatment according to a previous study.[32] In brief, mice (n = 6–8 in sham and CLP groups) were anesthetized with 4% isoflurane, after which a midline laparotomy of approximately 2 cm was performed to expose the cecum under sterile conditions. Half of the cecum-free end was ligated at the center and punctured with a 21-gauge needle between the ligation site and the end of the cecum, and then a small number of cecum contents was squeezed out. Then the cecum was gently repositioned, and the laparotomy site was then sutured. Sham-operated animals (Sham group) underwent laparotomy and bowel manipulation to expose the cecum without ligation and puncture. All mice were subcutaneously injected with 1 mL of saline. Following this, the mice were sacrificed and the serum and liver tissues were harvested for further analysis.

For antibiotic (ABX) treatment, the mice were administered antibiotics (ABX) (neomycin sulfate, 200 mg kg^{-1}; ampicillin, 200 mg kg^{-1}; metronidazole, 200 mg kg^{-1}; and vancomycin, 100 mg kg^{-1}), which were purchased from Sigma (St Louis, MO, USA), by oral gavage once each day for 5 days. The chemical reagent with doses of 30 mg kg^{-1} ML385 (HY-100523, MedChemExpress), an Nrf2 inhibitor, was intraperitoneally injected once a day for 7 days. Nobiletin (purity >95%) was purchased from MedChemExpress (NJ, USA). For nobiletin (NOB) administration (Fig. 1a), the mice were given 50 mg kg^{-1} nobiletin (HY-N0155, MedChemExpress) mixed with 0.5% carboxymethylcellulose sodium (CMC-Na) *via* oral gavage once a day for 7 days, and the control mice received an equivalent vehicle (Fig. 1b).

Sham group (6–8 mice per group): mice were subjected to oral gavage of the vehicle (sterile saline containing 0.5% CMC-Na) for 7 consecutive days. NOB group (6–8 mice per group): mice were subjected to oral gavage of NOB (50 mg

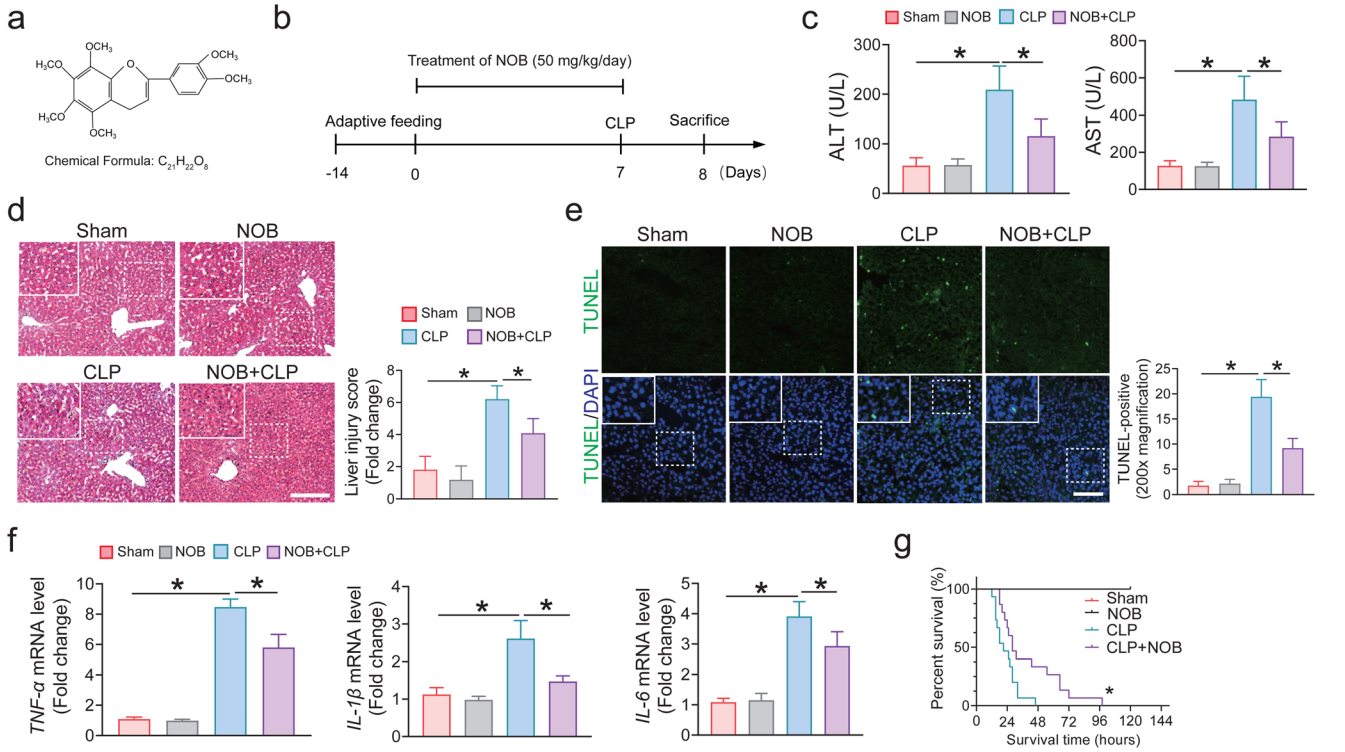

Fig. 1 NOB administration protects against sepsis-induced liver injury *in vivo*. Mice were administered 50 mg kg^{-1} NOB *via* oral gavage once a day for 7 days before CLP operation, and the degree of liver injury was evaluated. (a) Chemical structure of NOB. (b) Experimental design and timeline for the effects of NOB on liver injury induced by sepsis. (c) Relative plasma ALT and AST levels (n = 4). (d) H&E staining and the representative quantification on the right. Bar = 100 μm (n = 6–8). (e) Hepatic TUNEL staining and quantification of liver tissues. bar = 100 μm (n = 6–8). (f) mRNA levels of key proinflammatory factors in the liver by real-time PCR (n = 4). (g) Effect of NOB on the survival rate (n = 15). The results represent the mean ± SEM. *P < 0.05 determined by one-way ANOVA (Tukey's test) and log-rank test in G.

kg^{-1}, diluted with 0.5% CMC-Na) for 7 consecutive days. CLP group (6–8 mice per group): mice were subjected to oral gavage of the equivalent vehicle containing 0.5% CMC-Na for 7 days before CLP. NOB + CLP group (6–8 mice per group): mice were treated with NOB (50 mg kg^{-1}, diluted with 0.5% CMC-Na) by oral gavage for 7 days before CLP. NOB + ML385 + CLP group (6–8 mice per group): mice were subjected to oral gavage of NOB (50 mg kg^{-1}, diluted with 0.5% CMC-Na), and intraperitoneally injected with 30 mg kg^{-1} ML385 for 7 days before CLP. The other mouse experiment employed n = 6–8, while the experimental mice with the highest survival rate had a total n = 15.

2.2. Fecal microbiota transplantation

Fecal microbiota transplantation (FMT) was conducted as described previously.[18] Briefly, male C57BL/6J mice were administered with ABX by oral gavage once a day for 5 days to deplete the gut microbiota. Collected feces from CLP and NOB + CLP groups (donor mice) were resuspended in phosphate-buffered saline (PBS) at 0.125 g mL^{-1}. This suspension was administered to mice orally *via* a gastric gavage tube (0.15 mL) once a day. The compound feces of the CLP group mice were transplanted into the recipients (n = 6–8) by gavage (FMT-CLP), and the compound feces of the NOB + CLP group mice were transplanted into the other recipients (n = 6–8) *via* oral gavage (FMT-NOB) daily for 3 days. After 3 days, the mice underwent a CLP procedure and were euthanized 24 h later for further examination.

2.3 16S rRNA gene sequencing

Total genomic DNA from preoperative frozen cecum feces stored at −80 °C was extracted as previously described.[18] Next, the DNA extracted from the fecal contents was used to amplify the variable region 4 (V4) of the bacterial 16S rRNA gene using an Applied Biosystems 7500 Real-Time PCR System (Life Technologies Corporation, United States). The V4-16S rRNA gene was amplified by PCR with primer pairs (V4F, 5′-GTGTGYCAGCMGCCGCGGTAA-3′, and V4R, 5′-CCGGAC TACNVGGGTWTCTAAT-3′) and PCR amplification was performed with a reverse transcription enzyme (TOYOBO, Shanghai, China) using the following protocol: one cycle of 95 °C for 2 min, 28 cycles of 95 °C for 15 s, and 60 °C for 1 min to obtain melting curve data. Subsequently, the amplified products were quantified with QuantiFluor™ according to the manufacturer's recommendations.

All samples were sequenced on an Illumina Hiseq PE2500 sequencing platform by LC-Bio Technology Co., Ltd (Hang Zhou, Zhejiang Province, China). Quality filtering on the raw

reads was assessed under specific filtering conditions to obtain high-quality reads using the UPARSE pipeline. The alpha and beta diversities were performed by QIIME according to weighted and unweighted UniFrac distances. Next, Metastasis (version 20090414) and Linear discriminant effect size (LEfSe) software (version 1.0) were applied to analyze biomarkers in all groups. Tax-4Fun (version 1.0) was used to analyze The KEGG pathway analysis of the OTUs, and figures were drawn using the OmicShare tools.

2.4 Histological examination

4% paraformaldehyde was used to fix the mice's liver tissue, and then specimens of fresh liver tissues were embedded in paraffin blocks after dehydration. Next, these samples were sliced and stained using the experimental hematoxylin–eosin (H&E) protocol. The hepatic H&E scores were evaluated according to a previously described scoring system. Briefly, the histological assessment of liver damage included information, necrosis, and hepatocyte vacuolization. The scoring principle used a scale ranging from 0 to 3 (0 defined as absent and 3 defined as severe).

Terminal deoxynucleotidyl transferase dUTP mediated nick-end labeling (TUNEL) assay was performed according to the manufacturer's instructions. TUNEL-positive cells with nuclear staining were calculated in each 200× magnification field. The apoptotic cell was quantified using ImageJ software (Media Cybernetics, Inc., Rockville, MD, USA).

2.5 Survival study

A survival study was conducted as described previously.[18] 15 mice were included in each group for survival analysis. Additionally, the mice were observed every day for five days while the survival rate was noted. Every 6 hours for the first 2 days following CLP surgery, and then every 8 hours for the next 3 days. Kaplan–Meier analysis was used to assess the survival of mice.

2.6 Immunohistochemical staining

For immunochemical staining, paraffin sections (4 mm) were obtained according to the above protocol, and then sections were conducted following the standard immunostaining protocol. Liver sections were separated, rehydrated, and sequentially incubated with antibodies against 4-HNE antibodies (ab48506, Abcam). Finally, these dyed sections were observed with an optical microscope and quantified using ImageJ.

2.7 Immunofluorescence

The immunofluorescence assay was performed as in previous studies. Briefly, the liver paraffin sections were dewaxed, hydrated, antigen repaired, and circled. Then sections were incubated with anti-Gpx4 (67763-1-Ig, ABclonal), anti-Nrf2 (16396-1-AP, Proteintech), and anti-HO-1 (86806, Cell Signaling Technology) overnight at 4 °C. After extensive washing, the goat anti-rabbit secondary antibody was incubated at room temperature for 1 h. Finally, 4′,6-diamidino-2-phenylindole (DAPI) was used to label the nucleus.

2.8 Western blot analysis

Total protein was extracted using a protein extraction kit (Beyotime Biotechnology, China). Primary antibodies targeting Nrf2 (16396-1-AP, Proteintech), HO-1 (10701-1-AP, Proteintech), Gpx4 (67763-1-Ig, ABclonal), COX2 (12282, Cell Signaling Technology), and glyceraldehyde-3-phosphate dehydrogenase (60004-1-Ig, GAPDH) were used, and the secondary antibodies were horseradish peroxidase-labeled goat anti-rabbit antibodies (AS003, ABclonal) and anti-mouse antibodies (AS014, ABclonal). The band densities were standardized relative to the band density of GAPDH. Proteins in the western blot were quantified by measuring the density of blot bands *via* ImageJ software.

2.9 Transmission electron microscopy (TEM)

Fresh liver samples of 1–3 mm^3 were quickly harvested and then fixed with a fixative for TEM immediately. The tissue blocks were then post-fixed with 1% osmic acid, dehydrated with ethanol and acetone gradients, embedded in Epon-812 resin, and finally polymerized overnight. Next, the samples were cut into 70 nm-thick ultrathin sections according to the manufacturer's instructions. The sections were then observed, and photographs were captured under an H-7650 transmission electron microscope (Hitachi, Tokyo, Japan).

2.10 Biochemical analysis

Serum aspartate transaminase (AST) and alanine aminotransferase (ALT) levels were determined manually using an automatic biochemical analyzer (Jiancheng Bioengineering, Nanjing, China) based on the manufacturer's instructions.

2.11 Dihydroethidium staining

Dihydroethidium (DHE) (Invitrogen, MA, USA) was applied to measure hepatocellular reactive oxygen species (ROS) levels according to the manufacturer's protocol. Fresh frozen liver tissues were sliced into 8 μm thick frozen sections. Next, frozen sections were washed 3 times with PBS (PH 7.4) and then stained with the fluorescent probe DHE (2 μM) at 37 °C for 30 min. They were then washed with PBS and incubated with DAPI for 10 min. Images were captured immediately using fluorescence microscopy (Zeiss, Germany).

2.12 Gene expression analysis

The total RNA of liver tissues was extracted using the TRIzol reagent according to the manufacturer's instructions, and a reverse transcription enzyme (Vazyme, Nanjing, China) was used according to the standard protocol. Quantitative relative expression of targets was performed using Realtime PCR Master Mix (Vazyme, Nanjing, Japan) *via* an ABI 7500 real-time PCR system. The target gene primers in this study are listed in Additional file 1: Table S1.†

2.13 GSH and MDA measurements

A GSH assay kit (S0053; Beyotime, Shanghai, China) and a lipid peroxidation MDA assay kit (S0131; Beyotime) were

applied to measure liver GSH and MDA levels according to the manufacturer's instructions. The absorbance values at 412 nm and 535 nm were captured separately. Finally, the GSH and MDA levels were quantified following the standard curve.

2.14 Statistical analysis

All analyses were performed with GraphPad Prism 8 software, except the data of microbiota using multivariate and advanced statistical analysis as described above. All experimental data were presented as mean ± standard deviation (SD). Multigroup comparisons were performed by one-way analysis of variance (ANOVA) followed by the Tukey–Kramer multiple-comparison test. Student's *t*-test or Mann–Whitney Wilcoxon test was used to analyze the difference between two unpaired groups and a survival study was performed using the log-rank test. All data were representative of at least three separate experiments. A P-value < 0.05 was considered statistically significant.

3. Results

3.1 NOB administration protects against sepsis-induced liver injury *in vivo*

To determine the effect of NOB on SALI, mice were treated with NOB by daily oral gavage for 7 days before CLP. Blood samples were withdrawn from the eyeballs of mice for tests of ALT and AST, while the hemolysis samples were discarded, and $n = 4$ for each indicator. The liver tissues of these mice were used for qPCR examinations. As illustrated in Fig. 1c, NOB administration significantly attenuated the increase in ALT and AST levels, suggesting an improved liver function in the septic mice. Compared with the CLP group, NOB administration significantly attenuated SALI, as reflected by the hepatic H&E staining (Fig. 1d). Similarly, the liver histology TUNEL assay was used to identify the role of NOB in SALI mice, and the result demonstrated that NOB can significantly reduce the occurrence of cell death in SALI mice (Fig. 1e). NOB significantly ameliorated sepsis-induced inflammatory responses in liver tissues, reduced the mRNA levels of *TNF-α*, *IL-1β*, and *IL-6* (Fig. 1f). Moreover, NOB prolonged the survival times of CLP mice (Fig. 1g). Thus, these results suggest that NOB administration protects against liver injury induced by sepsis *in vivo*.

3.2 Oral gavage of NOB ameliorates sepsis-induced hepatic ferroptosis

Next, we explored whether NOB addressed the protective effects against hepatic ferroptosis induced by SALI. 4-HNE and MDA, which were principal aldehydic metabolites from the lipid peroxidation process, were assessed. As expected, oral gavage of NOB significantly reversed the increase in lipid peroxidation levels, which were observed in the CLP group (Fig. 2a and b). As shown in Fig. 2c, the GSH assays of liver tissue suggested that CLP treatment showed a lower level of GSH, while NOB administration could increase the GSH level. Next, we observed the structural change of mitochondria in liver tissues by TEM and surprisingly found that mitochondria in the CLP group appeared smaller than that in the sham group, with increased membrane density, which was the main feature of ferroptosis, while NOB administration ameliorated the mitochondrial damage (Fig. 2d). Given that the aberrant metabolism of iron is considered as an important ferroptosis factor,[33] we measured the iron level in the liver tissue. We validated that NOB reversed the increased iron levels in septic mice (Fig. 2h), suggesting that the Fenton reaction process could be inhibited by NOB administration. Furthermore, the immunofluorescence staining indicated that the CLP-induced ROS increase was significantly reversed by NOB (Fig. 2e and g). COX-2, also named prostaglandin-endoperoxide synthase 2 (PTGS2), serves as an identified marker of ferroptosis[34] and Gpx4 is considered an essential upstream ferroptosis mediator.[35] Compared with the CLP group, NOB administration increased the Gpx4 expression level and reduced the COX2 level (Fig. 2f and i). Together, our observations demonstrate that oral gavage of NOB ameliorates hepatic ferroptosis in septic mice.

3.3 NOB administration attenuates ferroptosis through Nrf2–Gpx4 signalling in SALI mice

To elucidate the underlying mechanism against hepatic ferroptosis by NOB in SALI mice, we further identified whether NOB attenuates ferroptosis by activating Nrf2 signalling. Heme oxygenase-1 (HO-1) is a critical downstream target of Nrf2 and exerts anti-oxidant stress and anti-inflammatory effects.[36] In detail, NOB replenishment increased Nrf2 and HO-1 levels by immunofluorescence staining, compared with the CLP group (Fig. 3a–d), suggesting that Nrf2/HO-1 signalling could be enhanced by NOB. To confirm that the beneficial effects of NOB administration against ferroptosis were Nrf2-dependent, the Nrf2 inhibitor ML385 was used to construct SALI mice (Fig. S1a†). Nrf2 inhibition abrogated the protective effects of NOB against the SALI (Fig. 3e and S1b†). Additionally, ML385 pretreatment significantly invalidated the anti-lipid peroxidation function of NOB, as indicated by a lower level of GSH and a high level of MDA in the livers of SALI mice (Fig. 3h and i). Subsequently, ML385 administration also significantly downregulated the Gpx4 level and upregulated the COX2 level compared with the NOB + CLP group (Fig. 3g). Collectively, these data suggest that NOB administration attenuates ferroptosis through Nrf2–Gpx4 signalling in SALI mice.

3.4 NOB changes the sepsis-shaped gut microbiota structure

We aimed to elucidate the underlying mechanism of the beneficial effects of NOB. Since the gut microbiota contributes to the sepsis progression,[37] we explored the potential regulation of gut microbiota composition by NOB in SALI mice and performed a 16S-rDNA gene sequencing on the feces samples of mice treated with CLP or NOB. There was a reduced alpha-diversity of bacteria in terms of Chao1 index, Shannon's index, and observed OTUs in the CLP-operated group compared to the sham group, while no significant difference was observed in alpha diversity between NOB-treated and CLP-treated groups (Fig. 4a–c). In contrast, NOB resulted in a higher Simpson index, whereas this was not the case in the NOB +

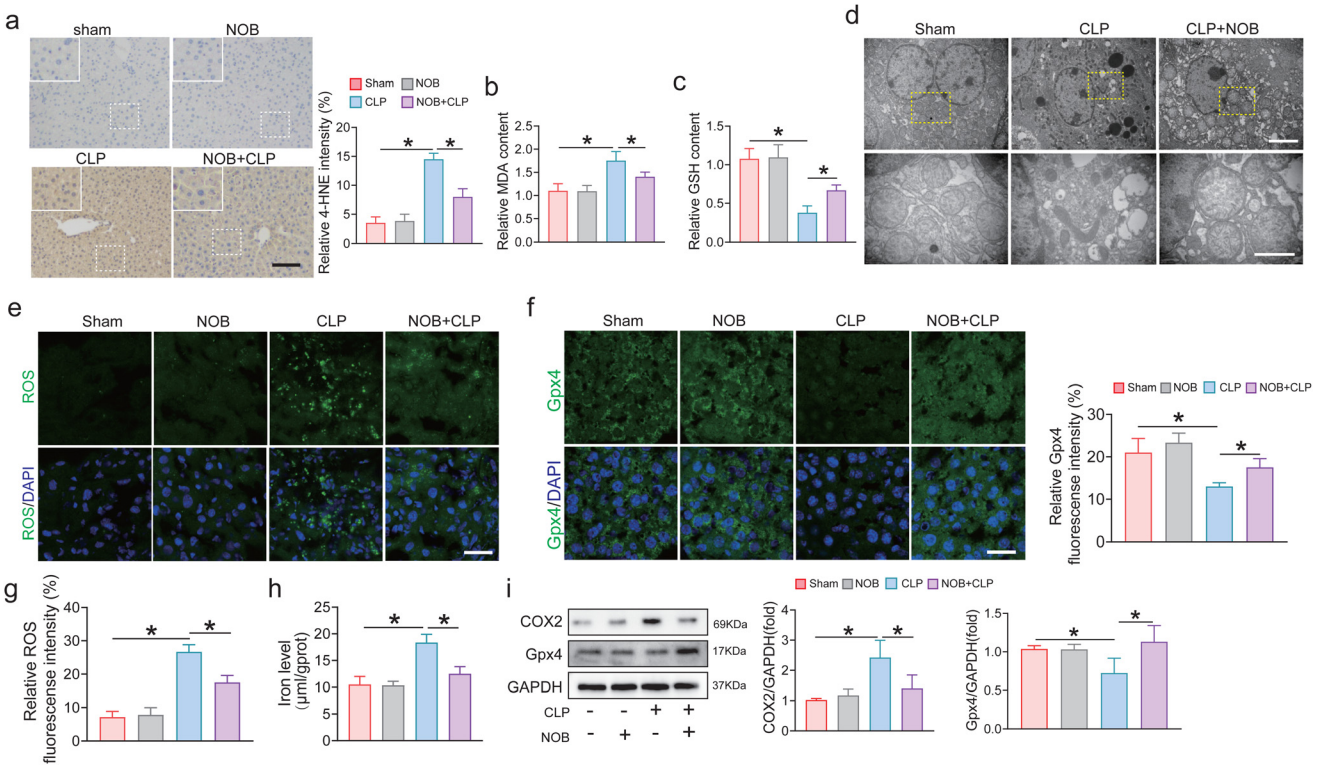

Fig. 2 Oral gavage of NOB ameliorates hepatic ferroptosis in septic mice. (a) Representative image and quantification of 4-HNE staining by immunohistochemical staining. Bar = 100 μm (n = 6–8). (b) Relative malondialdehyde (MDA) levels in liver tissues (n = 4). (c) Relative glutathione (GSH) levels in liver tissues (n = 4). (d) Representative images of the mitochondrial morphology in hepatocytes of liver tissues treated with or without NOB. (e and g) Representative image of fluorescent probe for ROS and its representative quantification by immunofluorescence staining. Bar = 100 μm (n = 6–8). (f) Relative protein levels of Gpx4 in the liver were measured by immunofluorescence staining. Bar = 100 μm (n = 6–8). (h) Relative iron levels of the liver tissues (n = 4). (i) Relative protein expression and quantification of Gpx4 and COX2 by Western blots (n = 4). Data are expressed as the mean ± SEM. *P < 0.05 was determined by one-way ANOVA (Tukey's test).

CLP group (Fig. 4d). The ratio of *Firmicutes*/*Bacteroidetes* slightly decreased in the CLP group compared with the controls at the phylum level, whereas NOB reversed the decreased *Firmicutes*/*Bacteroidetes* ratio in septic mice (Fig. 4e). Moreover, at the genus level, an increased abundance of *Ligilactobacillus* and *Dubosiella* was observed in the feces of the CLP group compared to that in the feces of the sham group, while NOB administration decreased *Dubosiella* and *Bacteroides* abundance, and increased the abundance of *Ligilactobacillus*, *Akkermansia*, and *Lactobacillus* in septic mice (Fig. 4f). Meanwhile, we also observed significant differences in the beta diversity of the samples in each operated group, as evidenced by a weighted principal coordinates analysis (PCoA) of the Binary Jaccard distance and ANOSIM analysis (Fig. 4g and h), suggesting that NOB might restructure bacterial composition despite the contrary influence of sepsis. Additionally, linear discriminant effect size (LEfSe) analysis indicated that specific bacterial lineages were distinguishable in NOB-treated mice compared with those in the CLP group, and the higher relative abundance of *Ligilactobacillus*, *Paramuribaculum*, *Akkermansia*, *Klebsiella*, *Lactobacillus, Erysipelatoclostridium*, *Muribaculum*, and *Parabacteroides* was statistically significant (Fig. 4i). Collectively, these results demonstrate that NOB administration modulates the composition of the gut microbiota in SALI mice.

3.5 The beneficial effects of NOB on sepsis progression are associated with the gut microbiome

To confirm whether NOB-induced modulation of the gut microbiota was essential for the beneficial effects on sepsis progression, a cocktail of broad-spectrum ABX was used to suppress or remove most of the gut microbes in CLP-operated mice. The mice were administered antibiotics by oral gavage once a day for 5 days before CLP operation (Fig. 5a). Accordingly, α and β diversity analysis showed that ABX treatment decreased the diversity of the gut microbiota in the NOB + CLP group, indicating that ABX treatment could effectively abolish the alteration of the gut microbiota induced by NOB (Fig. S1c–e†). Microbiota-depleted mice exacerbated the sepsis-induced liver injury, based on increased histopathological scores, serum ALT and AST levels, mitochondrial damage, and TUNEL-positive cells (Fig. 5b–e). In addition, ABX oral administration also increased significantly the mRNA expression of inflammatory factors *TNF-α*, *IL-1β*, and *IL-6* compared with the NOB + CLP group (Fig. 5f). Furthermore, ABX treatment showed a higher level of lipid peroxidation and iron and a lower level of GSH (Fig. 5g–j).

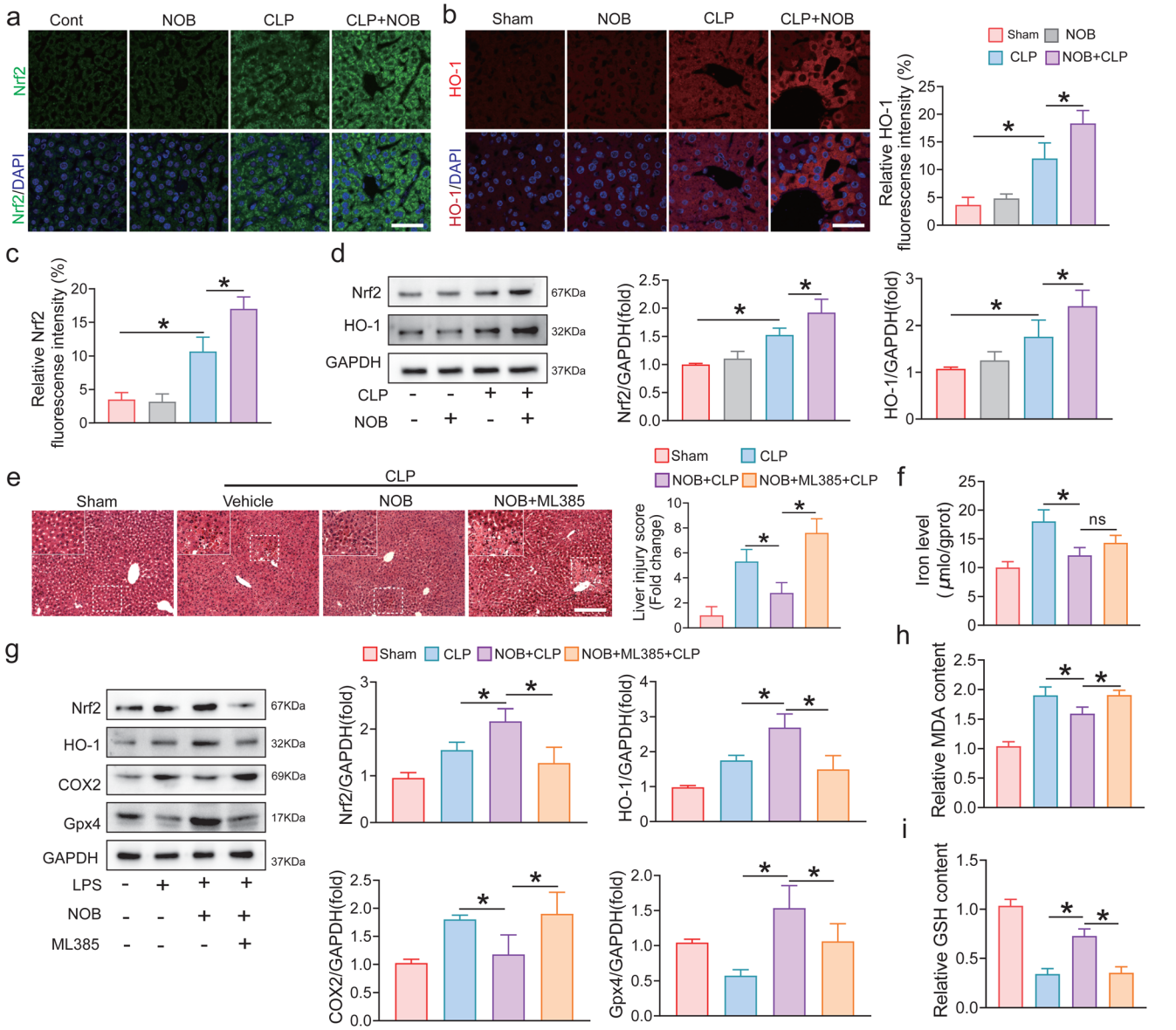

Fig. 3 NOB administration attenuates ferroptosis through Nrf2–Gpx4 signalling in SALI mice. (a and c) Relative protein levels of Nrf2 in the liver were measured by immunofluorescence staining. Bar = 100 μm (n = 6–8). (b) Representative image and quantification of HO-1 staining by immunofluorescence staining. Bar = 100 μm (n = 6–8). (d) Relative protein expression and quantification of Nrf2 and HO-1 by Western blots (n = 4). (e) H&E staining and the representative quantification on the right. Bar = 100 μm (n = 6–8). (f) Relative iron levels of the liver tissues (n = 4). (g) Relative protein expression and quantification of Nrf2, HO-1, Gpx4, and COX2 by Western blots (n = 4). (h) Relative MDA levels in liver tissues (n =4). (i) Relative GSH levels in liver tissues (n = 4). Data are expressed as the mean ± SEM. *P < 0.05, and ns indicates nonsignificant by one-way ANOVA (Tukey's test).

Consistently, the western blot results revealed that ABX treatment aggregated ferroptosis and activated Nrf2 signalling. Together, these findings indicate that NOB is probably a vital mediator of the gut microbiota and ameliorates ferroptosis in SALI mice through the gut–liver axis.

3.6 NOB attenuates sepsis-induced ferroptosis by modulating the gut microbiota

The FMT experiment was performed to explore the relationship between NOB-induced modulation of the gut microbiota and the protective effect against SALI. After treatment with an antibiotic cocktail once daily for 5 days to deplete the intestinal microbiota, the mice received feces from the CLP group or NOB + CLP group mice for 3 days (Fig. 6a). Our results have confirmed the success of FMT (Fig. S2a–i†). There was no appreciable difference in NOB levels in the feces between the NOB + CLP groups and the CLP groups by targeted liquid chromatography-tandem mass spectrometry analysis (LC-MS/MS) (Fig. S3†). Surprisingly, the mice that received feces of the NOB + CLP group exhibited lower liver damage than the mice that received feces from the CLP treatment group, as indicated by increased liver pathology scores, serum ALT and AST levels,

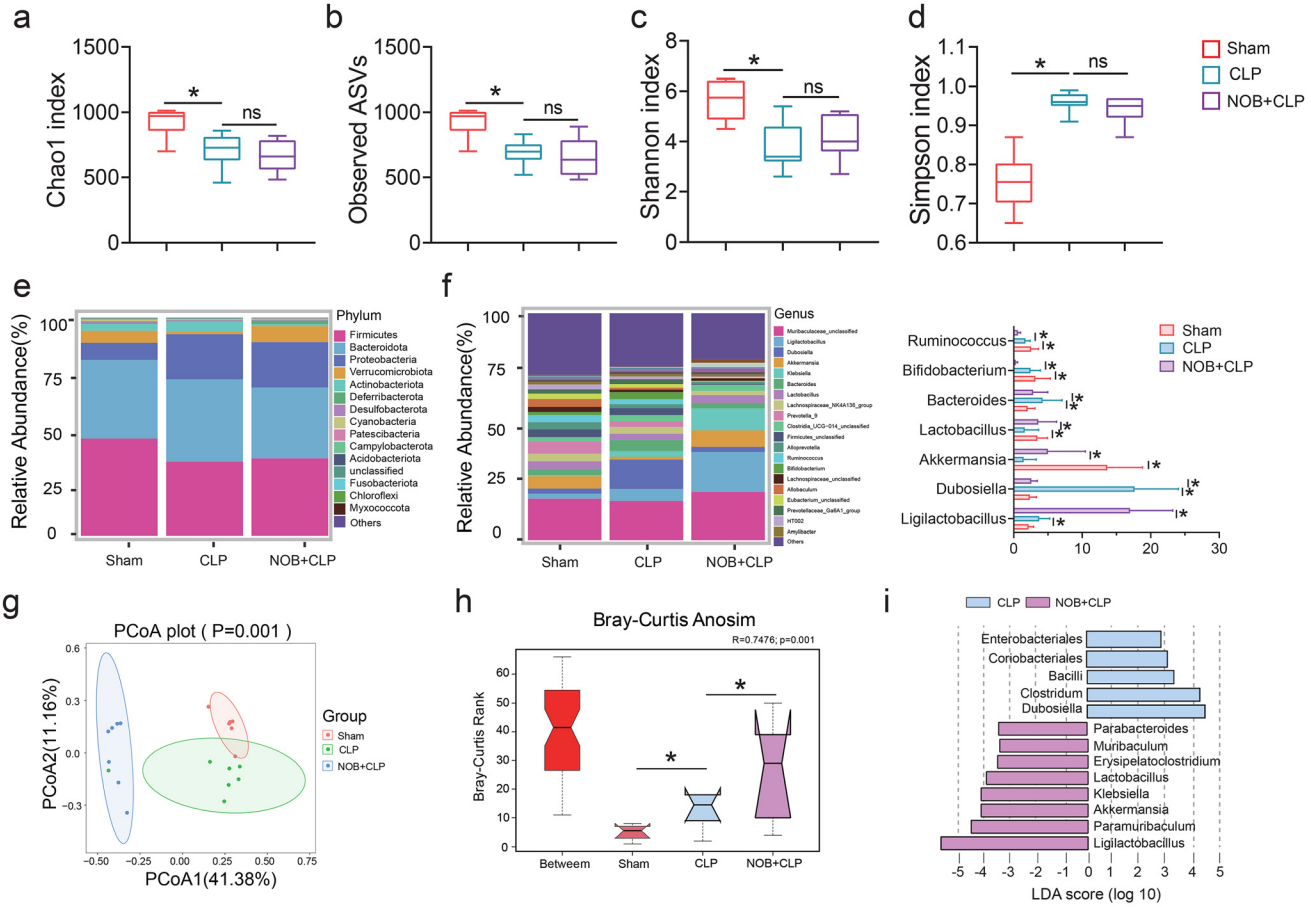

Fig. 4 NOB administration changes the sepsis-shaped gut microbiota structure. (a–d) Alpha diversity indices were accessed using Chao 1, observed OTUs, Shannon, and Simpson in gut microbiomes. (e and f) Relative abundance of the gut bacteria at the phylum and genus levels in each group. (g) The β-diversity of intestinal bacteria showed by the weighted uniFrac principal coordinates analysis (PCoA). (h) ANOSIM analysis on weighted UniFrac distances in feces. (i) The histogram of linear discriminant analysis (LDA) represents the enriched bacteria between the CLP and NOB + CLP groups. Data are expressed as the mean ± SEM. $*P < 0.05$, and ns indicates nonsignificant by one-way ANOVA (Tukey's test), Adonis analysis, and ANOSIM analysis in G and H.

mitochondrial damage, and TUNEL-positive cells (Fig. 6b–e). Next, we observed that the mRNA expression of inflammatory factors *TNF-α*, *IL-1β*, and *IL-6* decreased in mice that received feces from the NOB + CLP group compared to the mice that received feces from the CLP group (Fig. 6f), indicating that the anti-inflammatory activity of NOB partly depends on the gut microbiota. After FMT, the mice that received feces from the NOB + CLP group also showed markedly diminished ferroptosis and activated Nrf2 signalling (Fig. 6g–k). This suggested that NOB inhibited ferroptosis, at least partially, through Nrf2 signalling in SALI mice by modulating the gut microbiota. The above results indicate that NOB attenuates ferroptosis and inflammation in septic liver injury by modulating the gut microbiota.

4. Discussion

Recently, growing evidence has highlighted the cross-talk between the gut microbiota and sepsis.[38] There is convincing evidence indicating the potential of constituting effective and safe therapies for sepsis by targeting the intestinal microbiota.[39,40] However, the detailed roles of the intestinal microbiota during sepsis remain largely unknown, and effective therapeutic strategies for its clinical application are still lacking. It is well documented that NOB shows a protective effect on LPS-induced acute lung injury and may be a promising agent for sepsis treatment.[41] Notably, our study has demonstrated that NOB administration could attenuate ferroptosis through Nrf2–Gpx4 signalling in septic liver injury by modulating the gut microbiota.

NOB displays antioxidant and anti-inflammatory properties, which are reported to be implicated in reducing the risks of various diseases, such as anti-cancer, obesity, immunomodulatory and cardiovascular diseases.[42] In contrast to the existing studies, we focused on the effects of NOB on ferroptosis in SALI. Ferroptosis is a recently identified form of programmed cell death that is mainly driven by iron-dependent lipid peroxidation.[43] In a previous study, NOB ameliorated renal fibrosis

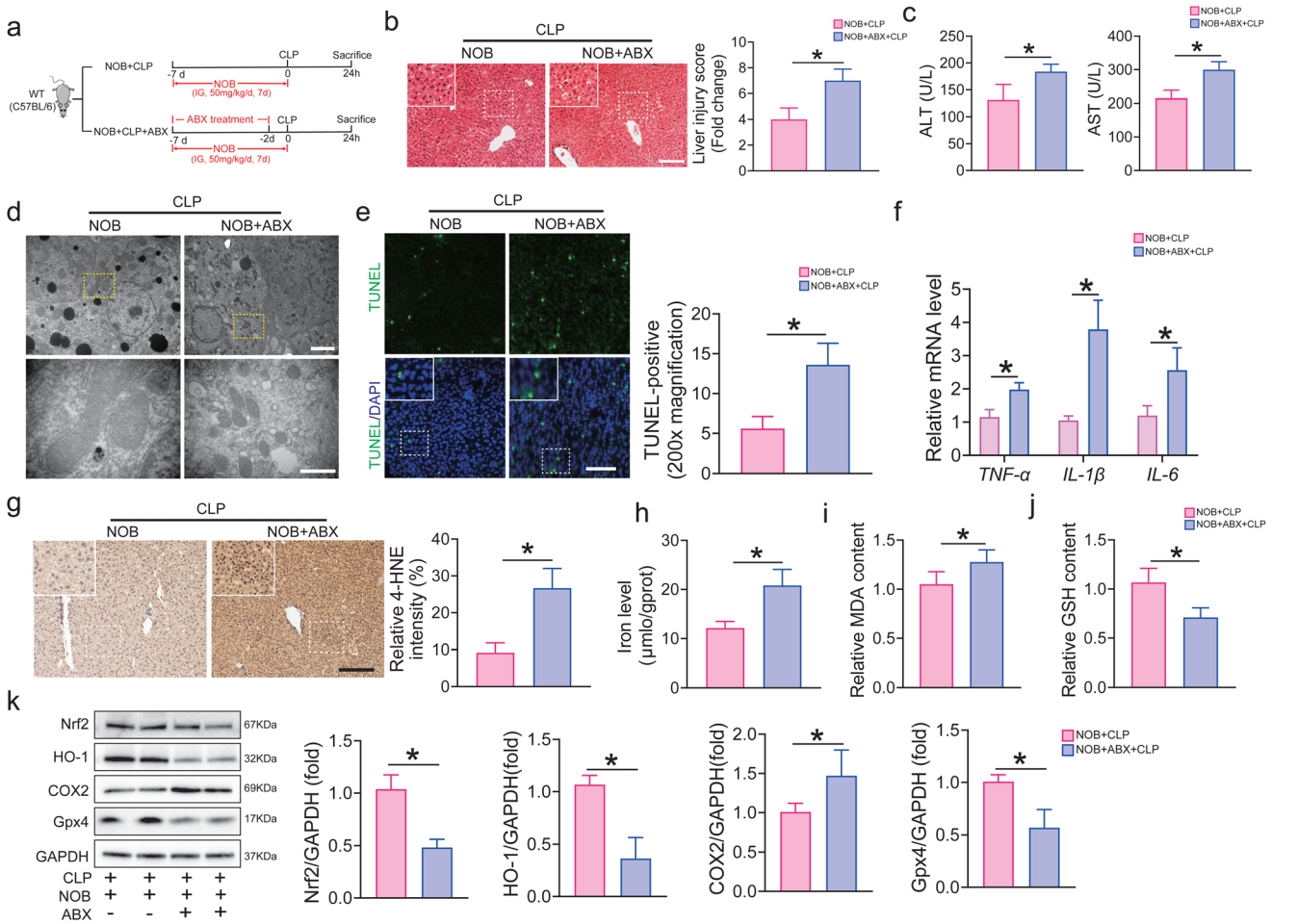

Fig. 5 The beneficial effects of NOB on sepsis progression are associated with the gut microbiome. (a) The antibiotic (Abx) experimental design and procedures for antibiotic (Abx) administration. (b) H&E staining and the representative quantification on the right. Bar = 100 μm (n = 6–8). (c) Relative plasma ALT and AST levels (n = 4). (d) Representative TRE images of hepatocytes after CLP. (e) Hepatic TUNEL staining and quantification of liver tissues. Bar = 100 μm (n = 6–8). (f) mRNA levels of key proinflammatory factors in the liver by real-time PCR (n = 4). (g) Representative image and quantification of 4-HNE staining by immunohistochemical staining. Bar = 100 μm (n = 6–8). (h) Relative iron levels of the liver tissues (n = 4). (i) Relative malondialdehyde (MDA) levels in liver tissues (n = 4). (j) Relative glutathione (GSH) levels in liver tissues (n = 4). (k) Relative protein expression and quantification of Nrf2, HO-1, Gpx4, and COX2 by Western blots (n = 4). Data are expressed as the mean ± SEM. *P < 0.05 was determined by one-way ANOVA (Tukey's test).

by repressing ferroptosis and oxidative stress in chronic kidney disease.[31] The application of NOB may, therefore, provide a novel therapeutic strategy for SALI, acting to inhibit ferroptosis. In the present study, we revealed for the first time that NOB can alleviate SALI by inhibiting hepatic ferroptosis *in vivo*. Mechanistically, we identified that NOB could reduce events characteristic of ferroptosis, including lipid peroxidation, GSH depletion, and excess iron accumulation. Moreover, the western blot results revealed that NOB administration increased the Gpx4 expression level and reduced the COX2 level compared with these CLP groups, suggesting that the oral gavage of NOB ameliorated hepatic ferroptosis in septic mice. Furthermore, we discovered that the function of NOB in hepatic ferroptosis inhibition was Nrf2-dependent. Our team unveiled that Nrf2 inhibition by ML385 treatment significantly invalidated the anti-lipid peroxidation function of NOB, downregulated the Gpx4 protein expression level, and upregulated COX2 levels. Intriguingly, ML385 treatment failed to reverse the iron level reduction caused by NOB replenishment in septic mice, suggesting that NOB may modulate the cytoplasmic iron level in an Nrf2-independent manner. It has been reported that NOB alleviates iron overload damage by increasing the activation of endogenous antioxidant enzymes in the vascular endothelium.[44] Thus, the relationship between NOB and iron metabolism in SALI mice requires further study. Consistent with other studies, we also demonstrated that key inflammatory cytokines such as *IL-1β*, *IL-6*, and *TNF-α*, in the liver were reduced following NOB pretreatment in SALI. Consequently, we suppose that NOB administration attenuates hepatic ferroptosis and inflammation through Nrf2–Gpx4 signalling in SALI mice.

Growing evidence has demonstrated the crucial role of the gut microbiota in sepsis pathophysiology and sepsis-related organ

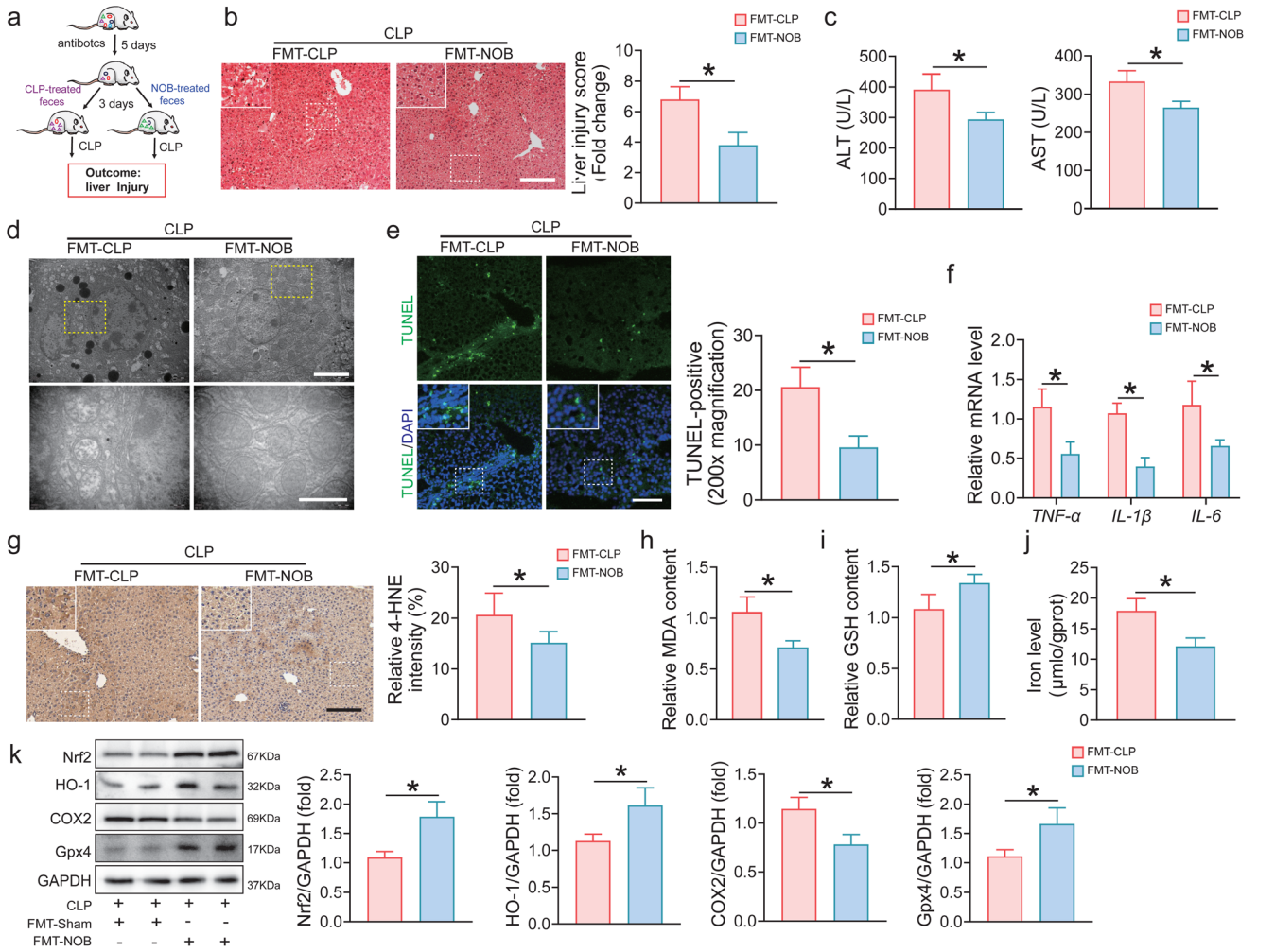

Fig. 6 NOB attenuates ferroptosis in septic liver injury by modulating the gut microbiota. (a) FMT experimental design and procedure. After treatment with an antibiotic cocktail once daily for 5 days, after which microbiota-depleted mice were subjected to CLP operation after 3 days of transplantation. (b) H&E staining and the representative quantification on the right. Bar = 100 μm (n = 6–8). (c) Relative plasma ALT and AST levels (n = 4). (d) Representative TRE images for hepatocytes after CLP. (e) Hepatic TUNEL staining and quantification of liver tissues. bar = 100 μm (n = 6–8). (f) mRNA levels of key proinflammatory factors in the liver by real-time PCR (n = 4). (g) Representative image and quantification of 4-HNE staining by immunohistochemical staining. Bar = 100 μm (n = 6–8). (h) Relative iron levels of the liver tissues (n = 4). (i) Relative malondialdehyde (MDA) levels in liver tissues (n = 4). (j) Relative glutathione (GSH) levels in liver tissues (n = 4). (k) Relative protein expression and quantification of Nrf2, HO-1, Gpx4, and COX2 by Western blots (n = 4). Data are expressed as the mean ± SEM. *P < 0.05 determined by Student's t-test.

dysfunction.[45,46] NOB is a polymethoxylated flavone extracted from the peel of citrus fruits,[47] and this strongly suggests that NOB may regulate the gut microbial community structure. Here, we observed that oral gavage of NOB did not increase the diversity and abundance of the intestinal microbiota during sepsis, while it promoted the integrity and function of the intestinal microbiome. In addition, we observed significant alterations in taxonomic unit abundance in CLP-treated mice compared with those in sham mice, whereas NOB administration reversed these changes. Accordingly, we found that NOB administration reversed the decreased *Firmicutes*/*Bacteroidetes* ratio in septic mice compared with the CLP group. Moreover, at the genus level, an increased abundance of *Ligilactobacillus*, *Akkermansia*, and *Lactobacillus*, and decreased abundance of *Dubosiella* and *Bacteroides* were observed under treatment with NOB when compared with that in the CLP-treated group. It is reported that *Ligilactobacillus* is conducive to the improved function of the intestinal microbiota and barrier.[48,49] However, we found that *Ligilactobacillus* expansion in the gut of septic mice was significantly enhanced by NOB, and the mechanism by which NOB enhances bacterial overgrowth needs to be further explored. More importantly, to explore whether the beneficial effects of NOB are dependent on alterations in the gut microbiota, a broad-spectrum antibiotic was used to investigate the causal role of the gut microbiota. As expected, we demonstrated that antibiotic treatment aggravated SALI, as evidenced by aggregated ferroptosis, and inhibited Nrf2 signalling. Together, our findings support that gut microbiota depletion partly abolishes the protective effects of NOB, indicating that NOB may attenuate SALI by modulating the gut microbiome.

Given that the most appropriate way for rebalancing the gut microbiota is fecal microbiota transplantation,[50] which has been identified as a therapeutic intervention to treat various diseases, we explored the effects of alterations in sepsis-induced gut dysbiosis influenced by NOB on the sepsis progression using FMT experiments. After FMT, the mice that received stool from the NOB + CLP group also showed markedly diminished ferroptosis and activated Nrf2 signalling compared with mice that received stool from the CLP treatment group, suggesting that NOB inhibited ferroptosis in SALI mice by modulating the gut microbiota. In addition, in the present study, recipients of feces from the NOB + CLP group showed a lower level of proinflammatory cytokines than CLP-treated feces recipients, which suggests that the anti-inflammatory activity of NOB is regulated by the gut microbiota. The above results indicate that NOB attenuates ferroptosis and enhances Nrf2 signalling in septic liver injury by modulating the gut microbiota.

However, several limitations are acknowledged in this study. First, given that the best method to identify the important role of the gut microbiota is to use germ-free mice, we found that the addition of broad-spectrum antibiotics at least partly abolished the protective effects of NOB against SALI. Therefore, additional studies are warranted to investigate the role of the gut microbiota in SALI using germ-free mice. Second, as NOB administration only partly reversed SALI, there must exist other potential mechanisms underlying the protective effects of NOB, including antioxidant properties or the restriction of apoptosis through Toll-like receptor 4 (TLR4) 4-mediated nuclear factor-κB (NF-κB) signalling pathways.[51] Third, we mainly revealed that NOB administration inhibited ferroptosis by repressing lipid peroxidation, and further investigations are required to understand the correlation between NOB and phospholipid substrates or iron metabolism.

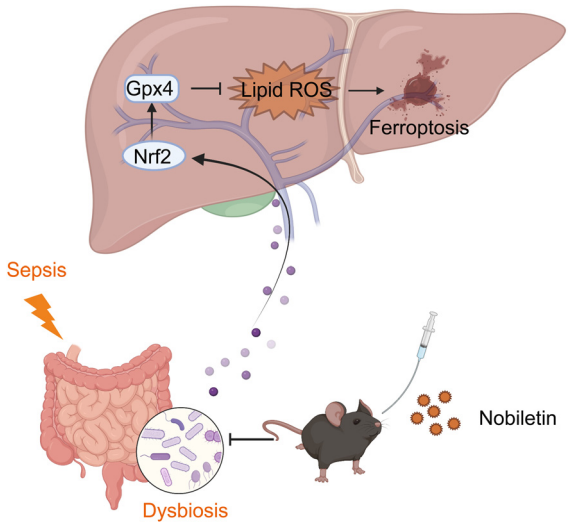

Fig. 7 Schematic diagram showing the protective effects of NOB against SALI. The beneficial effects of NOB administration may partly be dependent on alterations in the gut microbiota. Moreover, NOB attenuates hepatic ferroptosis through Nrf2–Gpx4 signalling in septic liver injury by modulating the gut microbiota.

5. Conclusions

In summary, we have shown that NOB protects against SALI. Mechanistically, the beneficial effects of NOB may be partly dependent on alterations in the gut microbiota. In addition, NOB attenuates ferroptosis and inflammation in septic liver injury by modulating the gut microbiota (Fig. 7). We also provide evidence that NOB exerts its protective effects, at least partially, through Nrf2–Gpx4 signalling. Clinically, NOB may be employed as a microbiome-based therapeutic approach for sepsis.

Author contributions

Wei Huang elaborated on the study design. Wei Huang, Hui Chen, and Qi He: conceptualization, methodology, investigation, and writing – original draft. Weidang Xie and Zanlin Peng: supervision, software, and data curation. Qiang Ma and Qiaobing Huang: methodology, supervision, and resources. Zhongqing Chen and Yanan Liu: project administration, funding acquisition, and writing – review & editing. All authors reviewed and approved the final manuscript.

Conflicts of interest

No potential conflict of interest was reported by all authors.

Acknowledgements

This work was supported by grants from the National Natural Science Foundation of China (82172181 and 81871604), Natural Science Foundation of Guangdong Province (2022A1515111071), and Certificate of China Postdoctoral Science Foundation Grant (2022M721503).

References

1 A. C. Liu, *et al.*, Sepsis in the era of data-driven medicine: personalizing risks, diagnoses, treatments and prognoses, *Briefings Bioinf.*, 2020, **21**, 1182–1195.
2 L. Evans, *et al.*, Surviving sepsis campaign: international guidelines for management of sepsis and septic shock 2021, *Intensive Care Med.*, 2021, **47**, 1181–1247.
3 M. Soni, M. Handa, K. K. Singh and R. Shukla, Recent nanoengineered diagnostic and therapeutic advancements in management of Sepsis, *J. Controlled Release*, 2022, **352**, 931–945.

4 J. Sun, *et al.*, Gut-liver crosstalk in sepsis-induced liver injury, *Crit. Care*, 2020, **24**, 614.
5 P. Strnad, F. Tacke, A. Koch and C. Trautwein, Liver - guardian, modifier and target of sepsis, *Nat. Rev. Gastroenterol. Hepatol.*, 2017, **14**, 55–66.
6 X. Wu, Y. Li, S. Zhang and X. Zhou, Ferroptosis as a novel therapeutic target for cardiovascular disease, *Theranostics*, 2021, **11**, 3052–3059.
7 Y. Sun, *et al.*, The emerging role of ferroptosis in inflammation, *Biomed. Pharmacother.*, 2020, **127**, 110108.
8 T. Hirschhorn and B. R. Stockwell, The development of the concept of ferroptosis, *Free Radicals Biol. Med.*, 2019, **133**, 130–143.
9 T. M. Seibt, B. Proneth and M. Conrad, Role of GPX4 in ferroptosis and its pharmacological implication, *Free Radicals Biol. Med.*, 2019, **133**, 144–152.
10 S. Wei, *et al.*,Serum irisin levels are decreased in patients with sepsis, and exogenous irisin suppresses ferroptosis in the liver of septic mice, *Clin. Transl. Med.*, 2020, **10**(5), e173.
11 J. Wang, *et al.*, YAP1 protects against septic liver injury via ferroptosis resistance, *Cell Biosci.*, 2022, **12**, 163.
12 M. Dodson, R. Castro-Portuguez and D. D. Zhang, NRF2 plays a critical role in mitigating lipid peroxidation and ferroptosis, *Redox Biol.*, 2019, **23**, 101107.
13 S. Huang, *et al.*, Hepatic TGFβr1 Deficiency Attenuates Lipopolysaccharide/D-Galactosamine-Induced Acute Liver Failure Through Inhibiting GSK3β-Nrf2-Mediated Hepatocyte Apoptosis and Ferroptosis, *Cell. Mol. Gastroenterol. Hepatol.*, 2022, **13**, 1649–1672.
14 C. Milani, *et al.*, The First Microbial Colonizers of the Human Gut: Composition, Activities, and Health Implications of the Infant Gut Microbiota, *Microbiol. Mol. Biol. Rev.*, 2017, **81**(4), e00036-17.
15 X. Zhang, *et al.*, The gut-liver axis in sepsis: interaction mechanisms and therapeutic potential, *Crit. Care*, 2022, **26**, 213.
16 B. W. Haak, H. C. Prescott and W. J. Wiersinga, Therapeutic Potential of the Gut Microbiota in the Prevention and Treatment of Sepsis, *Front. Immunol.*, 2018, **9**, 2042.
17 B. W. Haak, H. C. Prescott and W. J. Wiersinga, Therapeutic Potential of the Gut Microbiota in the Prevention and Treatment of Sepsis, *Front. Immunol.*, 2018, **9**, 2042.
18 S. Gong, *et al.*, Intestinal Microbiota Mediates the Susceptibility to Polymicrobial Sepsis-Induced Liver Injury by Granisetron Generation in Mice, *Hepatology*, 2019, **69**, 1751–1767.
19 H. Liang, *et al.*, Metformin attenuated sepsis-related liver injury by modulating gut microbiota, *Emerging Microbes Infect.*, 2022, **11**, 815–828.
20 F. Deng, *et al.*, The gut microbiota metabolite capsiate promotes Gpx4 expression by activating to inhibit intestinal ischemia reperfusion-induced ferroptosis, *Gut Microbes*, 2021, **13**(1), 1–12.
21 S. Liu, *et al.*, The gut microbiota metabolite glycochenodeoxycholate activates TFR-ACSL4-mediated ferroptosis to promote the development of environmental toxin-linked MAFLD, *Free Radicals Biol. Med.*, 2022, **193**, 213–226.
22 R. P. Dickson, *et al.*, Enrichment of the lung microbiome with gut bacteria in sepsis and the acute respiratory distress syndrome, *Nat. Microbiol.*, 2016, **1**, 16113.
23 M. Kumar, *et al.*, Increased intestinal permeability exacerbates sepsis through reduced hepatic SCD-1 activity and dysregulated iron recycling, *Nat. Commun.*, 2020, **11**, 483.
24 F. Lu, K. Inoue, J. Kato, S. Minamishima and H. Morisaki, Functions and regulation of lipocalin-2 in gut-origin sepsis: a narrative review, *Crit. Care*, 2019, **23**, 269.
25 B. He, *et al.*, The Small Molecule Nobiletin Targets the Molecular Oscillator to Enhance Circadian Rhythms and Protect against Metabolic Syndrome, *Cell Metab.*, 2016, **23**, 610–621.
26 X. Rong, *et al.*, Citrus peel flavonoid nobiletin alleviates lipopolysaccharide-induced inflammation by activating IL-6/STAT3/FOXO3a-mediated autophagy, *Food Funct.*, 2021, **12**, 1305–1317.
27 N. M. Morrow, *et al.*, Nobiletin Prevents High-Fat Diet-Induced Dysregulation of Intestinal Lipid Metabolism and Attenuates Postprandial Lipemia, *Arterioscler., Thromb., Vasc. Biol.*, 2022, **42**, 127–144.
28 S. Yuan, *et al.*, Hypoglycemic Effect of Nobiletin via Regulation of Islet β-Cell Mitophagy and Gut Microbiota Homeostasis in Streptozocin-Challenged Mice, *J. Agric. Food Chem.*, 2022, **70**, 5805–5818.
29 G. Kou, *et al.*, Nobiletin activates thermogenesis of brown and white adipose tissue in high-fat diet-fed C57BL/6 mice by shaping the gut microbiota, *FASEB J.*, 2021, **35**(2), e21267.
30 M. Zhang, *et al.*, Bidirectional interaction of nobiletin and gut microbiota in mice fed with a high-fat diet, *Food Funct.*, 2021, **12**, 3516–3526.
31 Y.-H. Lo, *et al.*, Nobiletin Alleviates Ferroptosis-Associated Renal Injury, Inflammation, and Fibrosis in a Unilateral Ureteral Obstruction Mouse Model, *Biomedicines*, 2022, **10**(3), 595.
32 M. Sun, *et al.*, p53 Deacetylation Alleviates Sepsis-Induced Acute Kidney Injury by Promoting Autophagy, *Front. Immunol.*, 2021, **12**, 685523.
33 Y. Yu, *et al.*, Hepatic transferrin plays a role in systemic iron homeostasis and liver ferroptosis, *Blood*, 2020, **136**, 726–739.
34 C. Chen, J. Chen, Y. Wang, Z. Liu and Y. Wu, Ferroptosis drives photoreceptor degeneration in mice with defects in all-trans-retinal clearance, *J. Biol. Chem.*, 2021, **296**, 100187.
35 Y. Zhang, *et al.*, mTORC1 couples cyst(e)ine availability with GPX4 protein synthesis and ferroptosis regulation, *Nat. Commun.*, 2021, **12**, 1589.
36 M. Ge, *et al.*, Brg1-mediated Nrf2/HO-1 pathway activation alleviates hepatic ischemia-reperfusion injury, *Cell Death Dis.*, 2017, **8**(6), e2841.

37 M. W. Adelman, *et al.*, The gut microbiome's role in the development, maintenance, and outcomes of sepsis, *Crit. Care*, 2020, **24**, 278.
38 W. D. Miller, R. Keskey and J. C. Alverdy, Sepsis and the Microbiome: A Vicious Cycle, *J. Infect. Dis.*, 2021, **223**, S264–S269.
39 H. Zhao, Y. Lyu, R. Zhai, G. Sun and X. Ding, Metformin Mitigates Sepsis-Related Neuroinflammation Modulating Gut Microbiota and Metabolites, *Front. Immunol.*, 2022, **13**, 797312.
40 X. Gai, *et al.*, Fecal Microbiota Transplantation Protects the Intestinal Mucosal Barrier by Reconstructing the Gut Microbiota in a Murine Model of Sepsis, *Front. Cell. Infect. Microbiol.*, 2021, **11**, 736204.
41 W. Li, *et al.*, Nobiletin-Ameliorated Lipopolysaccharide-Induced Inflammation in Acute Lung Injury by Suppression of NF-κB Pathway In Vivo and Vitro, *Inflammation*, 2018, **41**(3), 996–1007.
42 H. Wang, Y. Guo, Y. Qiao, J. Zhang and P. Jiang, Nobiletin Ameliorates NLRP3 Inflammasome-Mediated Inflammation Through Promoting Autophagy via the AMPK Pathway, *Mol. Neurobiol.*, 2020, **57**, 5056–5068.
43 C. Liang, X. Zhang, M. Yang and X. Dong, Recent Progress in Ferroptosis Inducers for Cancer Therapy, *Adv. Mater.*, 2019, **31**(51), e1904197.
44 Z. Wang, *et al.*, Nobiletin Regulates ROS/ADMA/DDAHII/eNOS/NO Pathway and Alleviates Vascular Endothelium Injury by Iron Overload, *Biol. Trace Elem. Res.*, 2020, **198**, 87–97.
45 S. M. Kim, *et al.*, Fecal microbiota transplant rescues mice from human pathogen mediated sepsis by restoring systemic immunity, *Nat. Commun.*, 2020, **11**, 2354.
46 H. Fang, *et al.*, Indole-3-Propionic Acid as a Potential Therapeutic Agent for Sepsis-Induced Gut Microbiota Disturbance, *Microbiol. Spectrum*, 2022, **10**(3), e0012522.
47 W. Liao, *et al.*, Enhancement of Anti-Inflammatory Properties of Nobiletin in Macrophages by a Nano-Emulsion Preparation, *J. Agric. Food Chem.*, 2018, **66**, 91–98.
48 C. Liang, *et al.*, Ligilactobacillus Salivarius LCK11 Prevents Obesity by Promoting PYY Secretion to Inhibit Appetite and Regulating Gut Microbiota in C57BL/6J Mice, *Mol. Nutr. Food Res.*, 2021, **65**(17), e2100136.
49 Y. Indo, *et al.*, Strains Isolated From the Porcine Gut Modulate Innate Immune Responses in Epithelial Cells and Improve Protection Against Intestinal Viral-Bacterial Superinfection, *Front. Immunol.*, 2021, **12**, 652923.
50 H. Antushevich, Fecal microbiota transplantation in disease therapy, *Clin. Chim. Acta*, 2020, **503**, 90–98.
51 Y. Wu, *et al.*, Nobiletin ameliorates ischemia-reperfusion injury by suppressing the function of Kupffer cells after liver transplantation in rats, *Biomed. Pharmacother.*, 2017, **89**, 732–741.